Journal of Applied Polymer Science

Rheological properties, cure characteristics, and morphology of acrylonitrile-based nanorubber modified epoxy

Nazli G. Ozdemir,[1] Tao Zhang,[1] Homayoun Hadavinia,[1] Ian Aspin,[2] Jian Wang[1]
[1]Kingston University, School of Mechanical and Automotive Engineering, London SW15 3DW, United Kingdom
[2]Cytec Industrial Materials, DE75 7SP, United Kingdom
Correspondence to: T. Zhang (E-mail: t.zhang@kingston.ac.uk)

ABSTRACT: This article investigates the effects of nano carboxylic acrylonitrile butadiene rubber (CNBR-NP) and nano acrylonitrile butadiene rubber (NBR-NP) on the rheological properties and cure characteristics of epoxy. Dynamic mechanical behavior of carbon fiber reinforced polymer composites (CFRP) with the nanorubber-modified matrices was also studied. Rheological study showed that NBR-NP blends attained lower viscosity in comparison to CNBR-NP blends and both systems exhibited shear-thinning behavior. Scanning electron microscopy (SEM) images revealed that CNBR-NP could be dispersed evenly within the epoxy matrix using industrial mixing process whereas partial agglomeration was observed in NBR-NP blends. The dynamic mechanical analysis (DMA) data showed that the addition of nanorubber has negligible effect on the glass transition temperature of the epoxy. The difference in the dispersion ability of these two nanorubbers in epoxy is related to the difference in van der Waals forces between single nanoparticles, the chemical formula and the polarity of the systems. © 2015 Wiley Periodicals, Inc. J. Appl. Polym. Sci. **2015**, *132*, 41911.

KEYWORDS: glass transition; nanostructured polymers; rheology; structure-property relations; synthesis and processing

Received 11 September 2014; accepted 24 December 2014
DOI: 10.1002/app.41911

INTRODUCTION

Epoxy resins are widely used in advanced carbon fiber reinforced polymer composites due to their outstanding mechanical performance, process-ability, and their chemical and wear resistance. However, these materials are relatively brittle which is detrimental to the engineering performance of the final structure. Due to the brittle nature of highly cross-linked epoxy resins, scientists have been toughening the formulations with nano- and micron-sized elastomeric particulates for more than 20 years. The addition of nanorubber to improve the fracture toughness of the epoxy matrix has been demonstrated by previous researchers.[1–5]

Nanorubber-modified epoxy blends play an important role in rubber industry. The morphology of the blends and its effect on the performances is significant for scientists. Therefore the microstructure for an optimum engineering performance and the ways to construct this microstructure are required. The morphology of the nanorubber/continuous polymer phase blends depends on the nanorubber concentration, compatibility between the blended phases and the processing parameters.[6] Most common method to obtain nanorubber blends is mechanical mixing where the dispersion phase is mixed with the continuous phase in mixing equipment. The mixing process is tricky due to the high viscosity of the nanorubber-modified blends. Achieving an even dispersion of nanorubber with low cost of energy and time is very important to both industry and academia and needs to be studied further.

As a matrix material, diglycidyl ether of bisphenol-A (DGEBA) epoxy cured with dicyandiamide (DICY) curing agent has been widely used in industry, especially in the preparation of prepregs and when toughened with different particles as curable structural adhesives between metallic plates.[7–11] Due to the complex structure and cross-linking mechanism of DICY curing agent, to our knowledge there is no work on nano acrylonitrile based rubber modification of DICY/epoxy systems in the literature.

The main challenge in incorporating soft nanoparticles into epoxy matrices is to increase the fracture toughness of the epoxy resin without sacrificing its basic properties such as glass transition temperature (T_g) and without increasing the viscosity considerably which will complicate the processing of composites. The variation in T_g can be interpreted in terms of the difference in cross-link densities of the matrix[12] and it gives an indication of the fundamental changes in polymer chain dynamics which is critical for many engineering applications.[13,14]

When toughening a resin system, the processing steps need to be optimized in order to achieve an even dispersion and to get the best efficiency for toughening. At this point, scientists

Table I. Formulations Used in Experimental Work, in phr (Per Hundred Resin)

Code	DGEBA	Curing agent	Accelerator	NBR-NP	CNBR-NP	Fumed silica
R	100	14	6	–	–	–
R/X FS	100	14	6	–	–	X
X CNBR-NP/R	100	14	6	–	X	–
X NBR-NP/R	100	14	6	X	–	–
E	100	–	–	–	–	–
EH	100	14	–	–	–	–
X CNBR-NP/E	100	–	–	–	X	–
X NBR-NP/E	100	–	–	X	–	–
X NBR-NP/EH	100	14	–	X	–	–

need to select the most suitable processing technique by studying the rheological characteristics of fluids with nanoparticle modification. This will determine the degree of dispersion of nanoparticles inside the epoxy matrix. The rheological analysis is also important to find out the relation between cross-linking and viscosity of the nanomodified system. So far, only few studies[15] have been reported on the rheological behavior of nanofluids. Key requirements for nanofluids are favourable rheological properties, flow behavior, and stability over a wide range of temperature to meet the industrial needs. This area needs to be studied further and this forms the primary motivation of this work.

In addition to the rheological properties, cure kinetics of the system needs to be studied in order to understand the effect of nanoparticles on the cross-linking phenomena and to choose the right cure cycle for the nanomodified resin.

In this research, epoxy matrices were modified with nano acrylonitrile butadiene rubber (NBR-NP) and nano carboxylic acrylonitrile butadiene rubber (CNBR-NP) by using a laboratory scale triple mill. Solid acrylonitrile butadiene rubber (NBR), with high acrylonitrile content is a suitable toughener. This is due to the high content of acrylonitrile imparting better compatibility between NBR and the epoxy resin.[16–18] Carboxylic acrylonitrile butadiene rubber (CNBR) is a modified NBR with carboxylic groups along the hydrocarbon backbone and imparts even better compatibility compared to NBR due to the presence of active polar groups on the particle surface.[19] CNBR is polar, reactive polymer that exhibits good compatibility with polar or nonpolar resins. Both ultrafine full vulcanized powdered rubbers have been prepared by cross-linking rubber latex using irradiation-curing method. To the best of our knowledge, very few studies have been reported on the toughening of epoxy matrix with acrylonitrile-based nanorubber materials[1] and no study on the rheological behavior and cure kinetics of this system was reported before. This forms the second motivation of this research.

This study constitutes a step behind mechanical characterization of these two novel nanomodified matrix materials helping to understand the effect of nanorubber on the rheological properties, the cure characteristics and the dynamic mechanical behavior of epoxy resin by considering the dispersion ability of them.

EXPERIMENTAL

Materials

The epoxy resin used was liquid DGEBA (Araldite LY1556) with epoxide equivalent weight of 188 and was supplied by Huntsman. DICY (Dyhard D50EP) was used as the curing agent and a difunctional urone (Dyhard UR500) was used as the accelerator, both supplied by AlzChem. Nano acrylonitrile butadiene rubber (NBR-NP) Narpow VP-401 (single particle size distribution, 100–150 nm; acrylonitrile content, 26 wt %), and nano carboxylic acrylonitrile butadiene rubber (CNBR-NP) Narpow VP-501 (single particle size distribution 50–100 nm; acrylonitrile content of 26 wt %) were received in powder form from SINOPEC, Beijing Research Institute of Chemical Industry (BRICI). Fumed silica (FS) received from Aerosil ($D_{50} = 1$ μm) was used in some of the formulations to modify the rheological behavior of the nanofluids for CFRP laminates processing. Carbon fibers were 2 × 2 Twill and 199GSM plies purchased from Sigmatex (UK) ltd. The matrix formulations used in this research work are given in Table I.

Sample Preparation, Nanorubber Toughened Resin Formulations

To improve the dispersion of nanoparticles in the matrix, different mixing techniques were investigated. The processing facility and the schematic of the processing techniques are shown in Figure 1.

CNBR-NP and NBR-NP modified resin matrices were prepared by the following procedures. In order to eliminate the absorbed moisture, the nanorubber was dried at ~70°C for 16 h in an oven. After drying, the nanorubber was dispersed in DGEBA epoxy and the final blend was speed mixed at 3500 rpm for 1 min using DAC 150.1 FVZ speed mixer. 0.25 to 1 phr (depending on the final viscosity of the blend) of Aerosil fumed silica was added to epoxy matrix in selected samples, which considerably increases the viscosity of the blends helping to prevent the leakage of resin matrix during curing of the CFRP laminates in autoclave under high pressures.

The final blend was triple milled for six times at room temperature (RT, 23°C). After first three times of triple milling, the blend was speed mixed at 2000 rpm for 6 min and visually inspected for translucency. This is a practical technique to

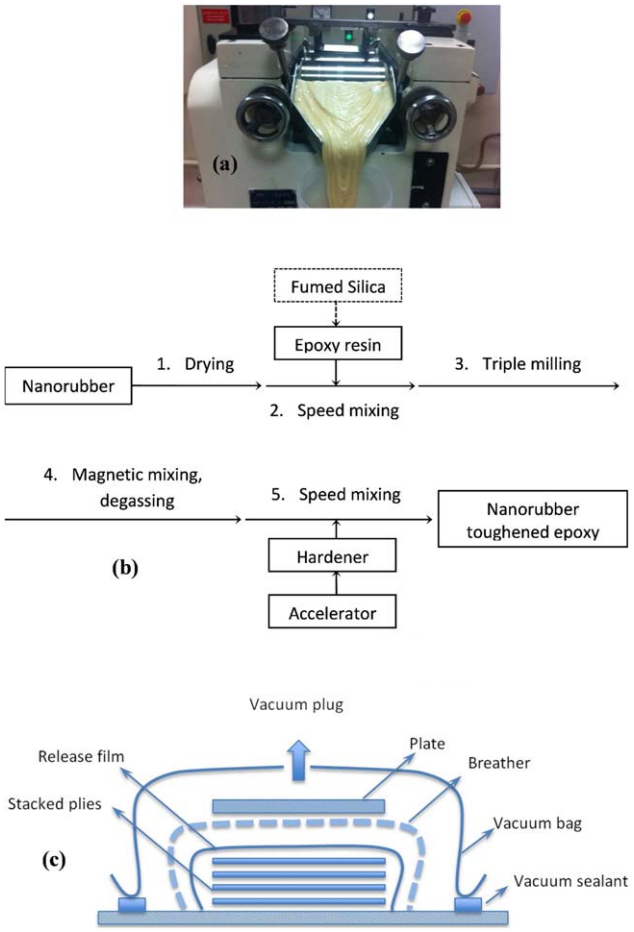

Figure 1. (a) Triple milling of nanorubber blends. (b) Schematic of the preparation of nanorubber toughened epoxy resin. (c) Vacuum bagged hand lay-up carbon plies ready to be autoclaved. [Color figure can be viewed in the online issue, which is available at wileyonlinelibrary.com.]

determine the degree of dispersion of the nanoparticles within the resin. When the nanoparticles are evenly dispersed in nano size the mixture does not reflect light and the blend attains translucency. If the blend was not translucent enough, it was triple milled for another three to four times at RT.

After the milling, the blend was magnetically stirred at a speed of 320 rpm and degassed at 70°C inside a glass flask for 16 h under vacuum. After degassing, the curing agent and accelerator were added and the final mixture was speed mixed at 2100 rpm for 6 min.

Sample Preparation, CFRP Laminates

Hand lay-up technique was used to produce the CFRP laminates. Eight unidirectional carbon plies with the nanorubber-toughened matrix were vacuum bagged and cured in an autoclave under a pressure of 6 bar. For morphological examination of the delamination surfaces, a piece of PTFE (polytetrafluoroethylene) release film was placed at the midplane of the laminate during hand lay-up in order to initiate crack propagation. The samples were heated to 120°C at a heating rate of 0.5°C/min and held for 1 h at this temperature before cooling down to RT at a cooling rate of 0.5°C/min. This cure condition was chosen from differential scanning calorimeter (DSC) studies performed in the dynamic mode, which revealed that almost all cure processes took place before 150°C. CFRP samples for dynamic mechanical analysis were cut from the cured laminates using a water jet cutting machine. Samples were carefully polished to remove surface defects.

CHARACTERIZATION

Morphological Study

Scanning electron microscopy (SEM) at secondary electron mode was used to verify the distribution of the nanorubber within the resin matrix. For this, the CFRP laminates were peeled along the PTFE film perpendicular to the delamination surfaces and the fracture surfaces were examined. The samples were vacuum coated with gold using a sputter coater. Images were taken using an accelerating voltage of 20–25 keV with a magnification between 90 and 2000 times.

Rheological Characterization, Steady Shear at Constant Rate

The processability of polymer matrix materials is directly related to their rheological property, which should be carefully controlled during processing. In the case of nanorubber toughened resin system, this property is sensitive to the composition and highly dependent on the dispersion state of the nanorubber.

Considering these facts, the rheological behavior of the neat epoxy (*E*) and the nanorubber toughened epoxy (*E*, CNBR-NP/*E*, and NBR-NP/*E* blends) at nanorubber loadings of 5/10/15/20 phr were analyzed at a strain of 0.1 and in the shear rate range of 1 to 10 s^{-1} using Bohlin Instruments C-VOR 200 rheometer. Three measurements were taken for each formulation.

Rheological Characterization, Oscillatory Mode

Dynamic rheological behavior of the nanorubber toughened resin blends (CNBR-NP/R and NBR-NP/R blends) was studied at 0.1 strain in the temperature range of RT to 200°C and at a heating rate of 2°C/min using Bohlin Instruments C-VOR 200 rheometer. In order to understand the difference in the cross-linking behavior with accelerator addition, NBR-NP with epoxy and DICY curing agent (X NBR-NP/EH) and the same formulation with accelerator (X NBR-NP/R) was studied.

Cure Analysis Using Differential Scanning Calorimetry (DSC)

Cross-linking activation energy (E_a) of the nanorubber-modified blends was studied using Flynn Wall Ozawa and Kissinger technique. These two methods were used in this study because they do not require knowledge of the reaction mechanism to quantify the kinetic parameters. For this; 5, 10, 15, and 20 phr NBR-NP and CNBR-NP toughened resin blends were prepared and heated at 5, 10, 15, and 20°C/min from RT to 300°C. The peak temperatures were recorded using differential scanning calorimeter Mettler Toledo DSC822.

Flynn-Wall-Ozawa Technique. The kinetics of cure reaction of epoxy resin was studied with Flynn Wall Ozawa technique, which is one of the non-isothermal DSC techniques.[20–22] All kinetic models start with the following equation:

$$da/dt = kf_{(a)} \quad (1)$$

where da/dt is the instant cure rate, a is the conversion ratio at time t, k is the rate constant (which depends on the

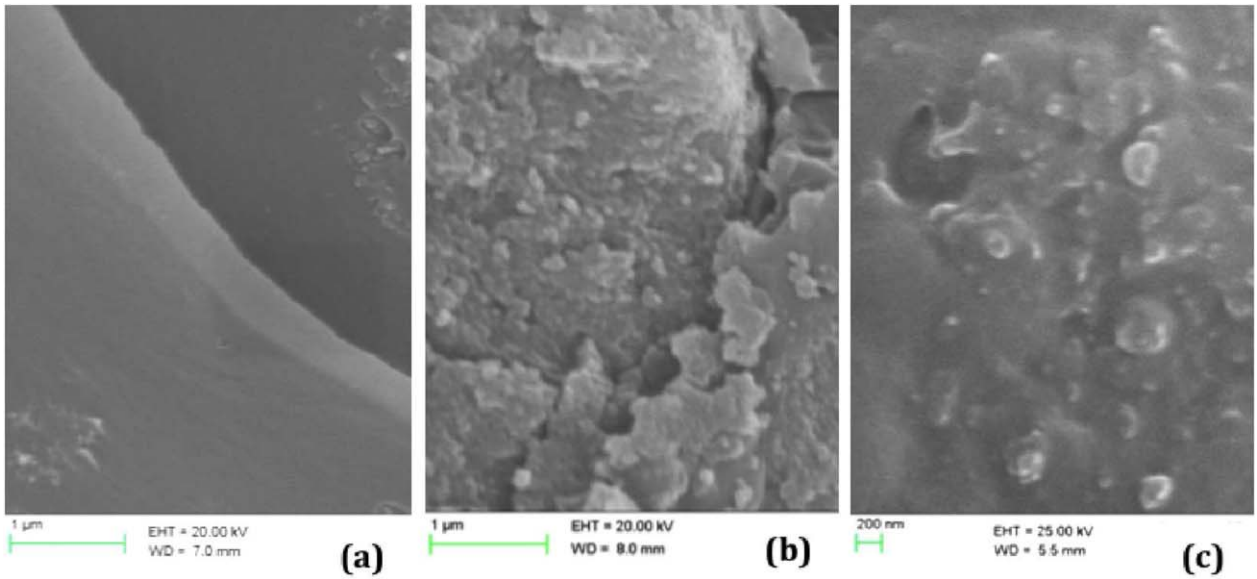

Figure 2. SEM images of (a) R sample, (b) 20CNBR-NP/R sample, (c) 20NBR-NP/R sample. [Color figure can be viewed in the online issue, which is available at wileyonlinelibrary.com.]

temperature T), $f_{(a)}$ is a functional term of a that depends on the reaction mechanism. The Arrhenius equation is as follows:

$$k = A \exp(-E_a/RT) \quad (2)$$

Based on Doyle's approximation,[23] Ozawa method is expressed as:

$$\ln(\beta) = \text{Const.} - 1.052E_a/RT_p \quad (3)$$

where β is the heating rate, T_p is the temperature at which da/dt is maximum, E_a is the activation energy, R is the universal gas constant. A plot of $\ln(\beta)$ versus $1/T_p$ gives a straight line with a slope of $1.052E_a/R$.

Kissinger Technique. According to the Kissinger method, the activation energy can be obtained from the maximum reaction rate where $[d(da/dt)]/dt$ is zero at a constant heating rate. The resulting relation can be expressed as:

$$d[\ln(\beta/T_p^2)]/d(1/T_p) = -E_a/R \quad (4)$$

Therefore a plot of $\ln(\beta/T_p^2)$ versus the reciprocal of T_p gives the activation energy E_a without the need to make any assumption about the conversion dependent function. Both Kissinger and Flynn Wall Ozawa methods assume that the DSC exothermic peak is isoconversional and that its value is independent of the heating rate.

Dynamic Mechanical Analysis (DMA)

The glass transition temperature of the nanoparticle toughened CFRP laminates was determined by dynamic mechanical thermal analysis testing by using a DMA Q800 dynamic mechanical analyzer. Laminates with dimensions of 50 × 10 × 2 mm were tested under three point bending mode at a fixed frequency of 1 Hz. The storage modulus, loss modulus and tan δ were measured as a function of temperature for the temperature range 20 to 200°C at a heating rate of 2°C/min. The glass transition temperature was determined as the maximum stationary point of the tan δ versus temperature curve. The data is based on an average of three experiments.

RESULTS AND DISCUSSION

Morphology

The fracture surfaces of the CFRP laminates with neat resin matrix and nanomodified matrices were examined using SEM. The morphological differences in the two-nanorubber systems arise from the dissimilarity in cross-linking density and the size of the rubber domains.

Figure 2 represents the fracture surface of the nanorubber-modified matrices. In Figures 2(a) and 3(a) the glassy fracture surface of the neat resin sample represent a typical brittle fracture. This is an indication that no visible plastic deformation occurred during fracture. Figure 2(b,c) shows that both CNBR-NP and NBR-NP were dispersed evenly in the highest rubber concentration samples. CNBR-NP has diameters less than 100 nm [Figure 2(b)]. However, NBR-NP showed slight agglomeration and the particle size is larger than that of CNBR-NP, in the range of 100 to 500 nm [Figure 2(c)]. De-bonding of nanorubber was observed in wide aspects in both nanorubber formulations. Due to this reason, voids within the resin structure were easily noticeable in all of the nanotoughened formulations.

Figure 3 represents the images of the matrices between the carbon fibers. In this figure, the black dispersed phases are the holes from where the nanorubbers have de-bonded and the light gray continuous phase is the resin matrix. In Figure 3(b–d), the spherical holes can be observed within the fracture surface of the CNBR-NP modified matrices. The holes have a diameter of 50 to 100 nm and they are dispersed evenly within the structure independent of the nanorubber concentration. The hole and particle diameter in CNBR-NP formulations is in the same range which indicates that cavitation and plastic void-growth

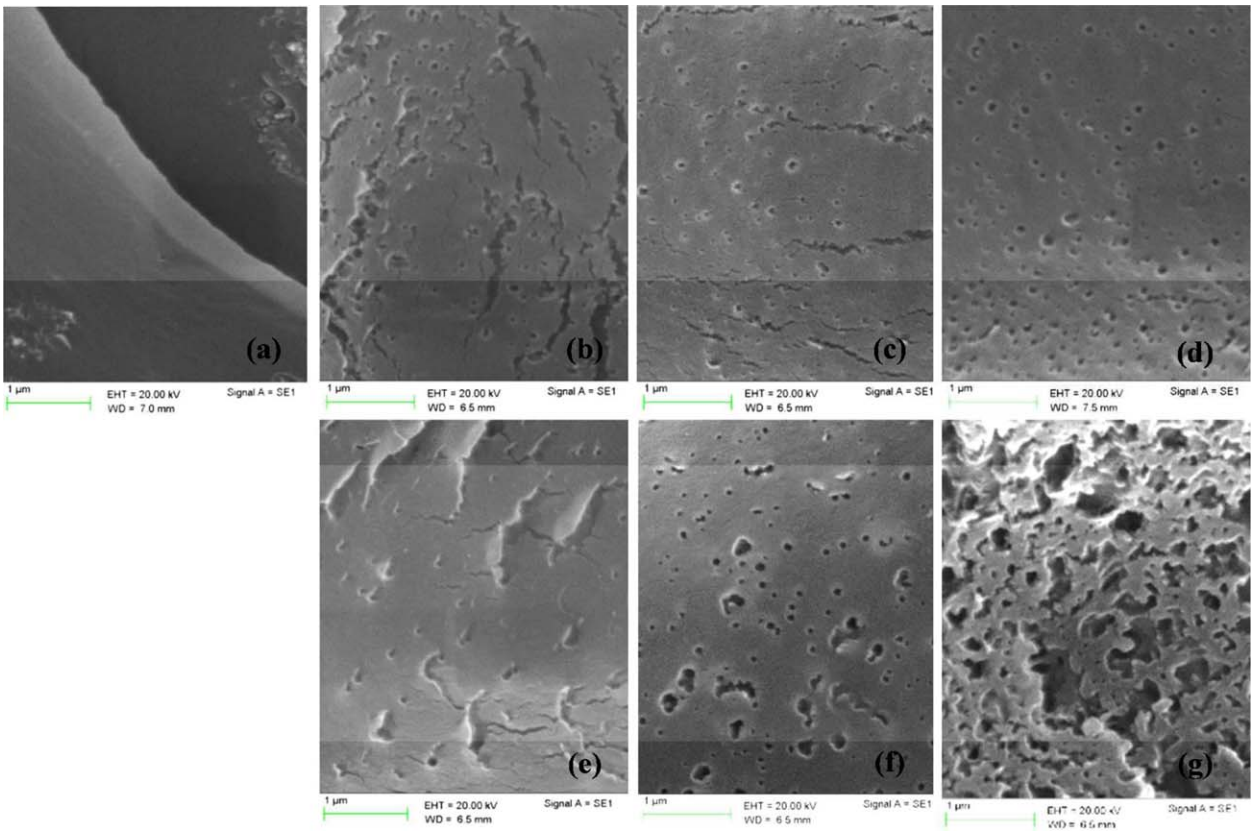

Figure 3. SEM images of (a) R sample (b) 5CNBR-NP/R sample, (c) 15CNBR-NP/R sample, (d) 20CNBR-NP/R sample, (e) 5NBR-NP/R sample, (f) 15NBR-NP/R sample, (g) 20NBR-NP/R sample. [Color figure can be viewed in the online issue, which is available at wileyonlinelibrary.com.]

did not happen. The holes are protuberant shape, which indicates that the particles and the matrix have a good adhesion. It is seen that by increasing the nanorubber loading, the number of holes per unit area and the hole diameter increase. However, it is seen in Figure 3(d) that the hole and particle sizes are still in nanorange in the highest nanorubber concentration sample.

It can be seen from Figure 3(e–g) that the fracture surfaces of the NBR-NP toughened CFRP laminates are relatively rough and the holes from where the NBR-NP have de-bonded have a larger diameter and the diameter increases with an increase in nanorubber loading. When the blend ratio of NBR-NP/resin is 5/100 as in Figure 3(e), NBR-NP is finely and uniformly dispersed in resin as spherical holes with the size close to its original particle size, 100 to 150 nm. However, as the blend ratio of NBR-NP to resin increases, NBR-NP start to agglomerate. Correspondingly, the size of the holes become larger and the shapes of dispersion evolve from sphere into strip. As a consequence, "network-like" structure is observed in Figure 3(g). The surfaces of the holes from where the particles were pulled out are comparably smooth which also suggests a relatively poor interface between the epoxy matrix and the particles. Some of the holes have a deformed-elliptical shape as in Figure 2(e–g), which may be the result of high shear during processing when NBR-NP was broken by shear stresses into irregular particles.[24] This means that NBR-NP cannot exhibit sufficient hardness and rigidity to resist being melted, compressed and flattened under the pressures and temperatures applied during the processing and curing of the samples. As a result, plasticization was inevitable within its formulations. The lower modulus and good deformability of NBR-NP impair dispersion because the higher shear force around NBR-NP agglomerates could not be generated according to traditional stress transfer theory.[25]

In powder form both nanorubbers are in clustered form. However when dispersed in the resin, using different dispersion techniques such as triple mill and high speed mixing, the rubber agglomerates can be broken down into even smaller diameters. Compared with CNBR-NP, the dispersion of NBR-NP in resin is poor, and partial agglomeration takes place at higher nanorubber concentrations.

The difference in efficiency of dispersion is due to the difference in the polarity, surface tension energy and the chemical formulations of the nanorubber systems. In a way the carboxylic group of CNBR-NP enables better dispersion within DGEBA matrix by providing additional network of ionic bonds.[26] The filler-filler interaction and the filler-rubber interaction predominate the dispersion besides the processing parameters.

Rheological Characterization, Steady Shear at Constant Rate

Rheological measurements of the nanofluids were carried out to characterize the nanofluid. Figure 4(a,b) shows the viscosity

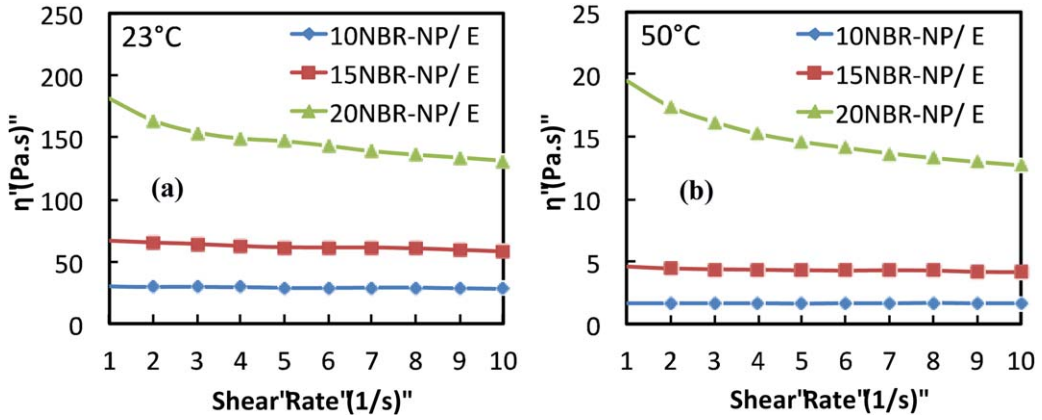

Figure 4. Viscosity (Pa s) vs. shear rate (s^{-1}) for (a) NBR-NP/E blends at 23°C (b) NBR-NP/E blends at 50°C. [Color figure can be viewed in the online issue, which is available at wileyonlinelibrary.com.]

versus shear rate of NBR-NP/E blends (NBR-NP modified DGEBA epoxy blends) at 23°C and 50°C. It is clear that the viscosity of the nanofluids is greater than that of the neat epoxy. The nanofluid viscosity increase with increasing nanorubber loading and decrease with an increase in temperature owing to the fact that the kinetic energy stored within the system increases and as a result the mobility of the polymer chains and nanoparticles increase.[27]

The viscosity versus shear rate of the CNBR-NP and NBR-NP toughened DGEBA epoxy blends (CNBR-NP/E and NBR-NP/E formulations) and the neat epoxy at RT are given in Figure 5(a,b). In these figures it is clear that the viscosity of the system increases consistently with nanorubber loading. The increase is much greater in CNBR-NP modified epoxy blends than in NBR-NP modified epoxy blends. This is due to the uniform dispersion of nanoparticles within CNBR-NP blends, which increases interfacial adhesion area between the resin and nanorubber particles whereas partial agglomeration was observed in SEM images of NBR-NP blends and resulted in lower interfacial adhesion area.

The rheological behavior of the blends was modeled by power law model with two fitting parameters: power law index (n) and consistency index (K). A power law fluid is a type of generalized Newtonian fluid for which the shear stress τ is given by:

$$\tau = K\dot{\gamma}^n \tag{5}$$

According to the power law model,

$$\eta = K\dot{\gamma}^{n-1} \tag{6}$$

where η is the viscosity and $\dot{\gamma}$ is the shear rate. Power law index n is an indication of the rheological behavior. If n is smaller than 1, the fluid acts like a shear thinning fluid. In the shear rate range of 1 to 10 s^{-1} and under the conditions of this work, the epoxy resin is a Newtonian fluid possessing an n value of 1, which means that the relation between the shear stress and the shear rate is linear yielding a constant coefficient of viscosity.

In order to characterize the rheological properties of the nanofluids, the logarithm of the shear stress was plotted against the logarithm of the shear rate. The slope and the intercept of the fitted line yield the power law index (n) and the consistency index (K) of the nanofluids respectively. The relevant equation is as below:

$$\log(\tau) = n\log(\dot{\gamma}) + K \tag{7}$$

The plots of log (shear stress (Pa)) versus log (shear rate (1/s)) for both nanorubber systems are given in Figure 5(c,d) together with the fitted lines. In Figure 5(e), for both nanorubber-toughened epoxy systems after about 5 phr of nanorubber toughening there is a tendency towards shear thinning. In other words the nanofluid gains a stronger shear thinning with an increase in nanoparticle concentration. The decrease in power law index (n) is steeper for CNBR-NP blends than that for NBR-NP blends indicating the stronger influence of CNBR-NP on the viscosity of the resin. The particle content in suspensions clearly influences the rheological behavior of these two nanorubber blend systems.

Quemada[28] proposed that the structure breakdown is the reason for shear thinning in non-Brownian suspensions. The higher the nanorubber content in the system, the more aggregates in the system due to a creation of excess surface area, the more susceptibility to break and the more shear thinning. Respectively fluidity of the system increases due to a decrease in the hydrodynamic forces between the particles.[29] Due to dissolution of 0.008 wt % of NBR-NP within the epoxy matrix (see Dynamic Mechanical Analysis) and the partial agglomeration, CNBR-NP when dispersed in epoxy resin at the same loadings had higher numbers of phase-separated particles with higher interfacial adhesion area resulting in higher viscosity and greater shear thinning.

The higher viscosity of CNBR-NP/E blends as matrix material eased the processing of CFRP since the leakage of resin when autoclaved under high processing pressures can be avoided. However, for NBR-NP modified resin blends, in order to achieve the same processing viscosity, fumed silica needs to be used.

This initial rheological characterization study was used as a guide for the processing of CFRP with nanorubber modified resin as matrices.

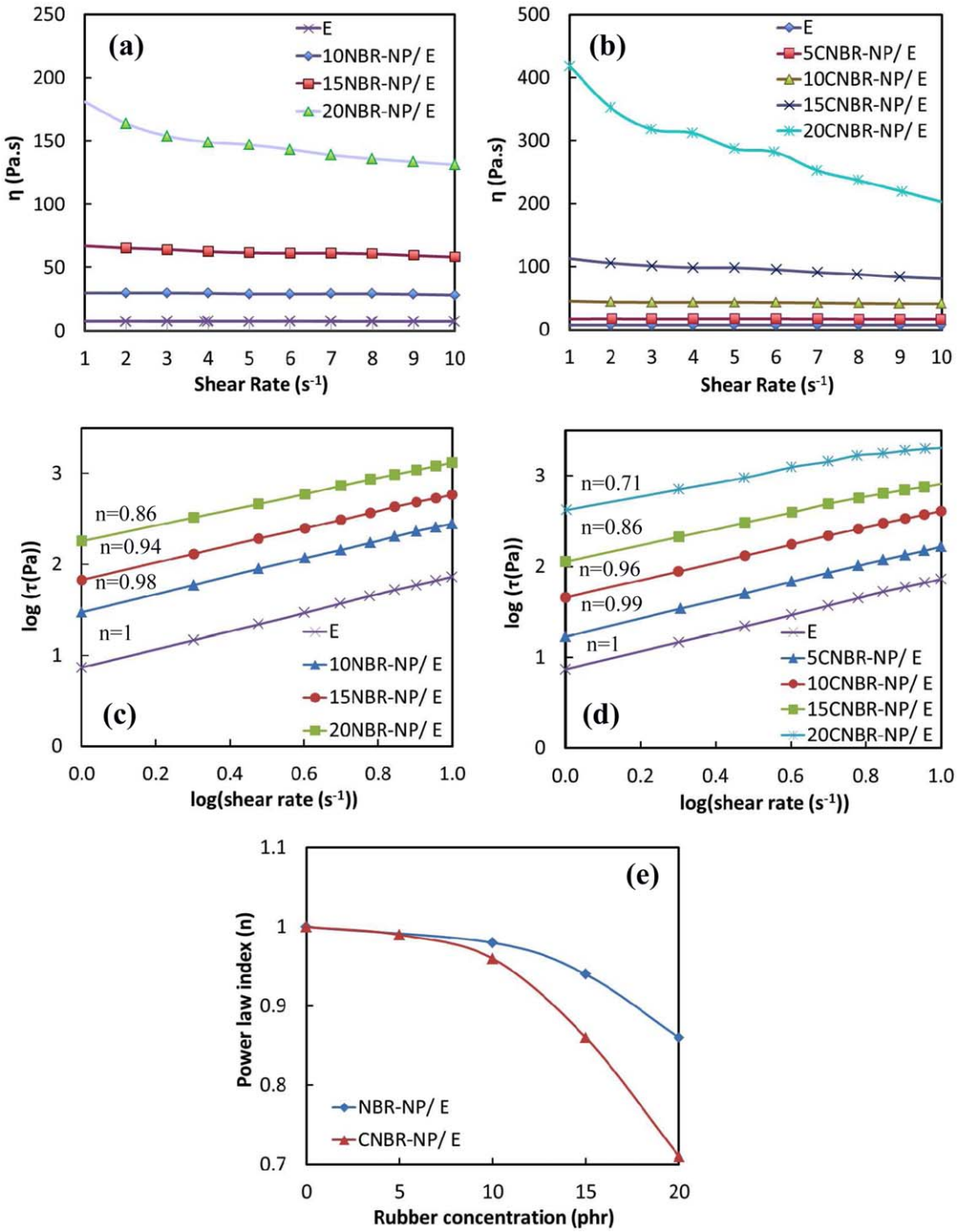

Figure 5. Viscosity (Pa s) vs. shear rate (s^{-1}) for (a) NBR-NP/E at RT, (b) CNBR-NP/E at RT, (c) log (τ (Pa)) vs. log (shear rate (s^{-1})) for NBR-NP/E, (d) CNBR-NP/E blends (τ = shear stress), (e) Power law index (n) vs. nanorubber concentration (phr). [Color figure can be viewed in the online issue, which is available at wileyonlinelibrary.com.]

Rheological Characterization, Oscillatory Mode

Rheological measurements of the nanofluids were carried out to characterize the cross-linking phenomena. The viscosity of the nanofluids decreases constantly with an increase in temperature and the internal energy stored within the system indicating the higher mobility of polymer chains and nanoparticles. At some point when the temperature has reached a high value the viscosity suddenly increases indicating the start of cross-linking of the chains or in other words cure of the system. These stages of rheological behavior are given in Figure 6. The cross-linking temperature was taken as the point where the continuous increase in viscosity was observed. The extracted cross-linking temperatures using this method are given in Table II.

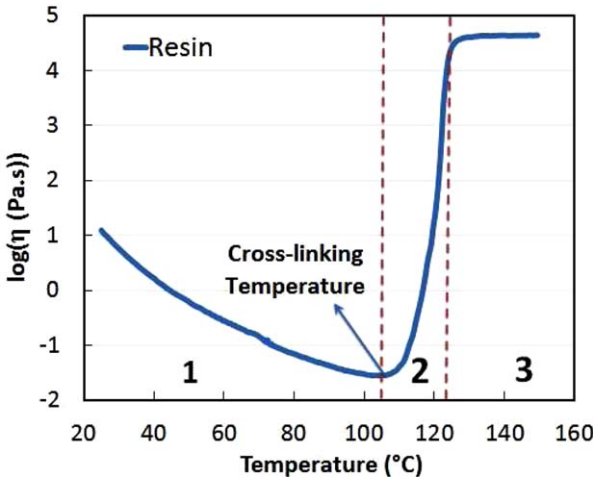

Figure 6. Rheological behavior of neat resin, first stage decrease in viscosity with increase of internal energy stored within the system, second stage cross-linking of the polymer resulting in a constant increase in viscosity, third stage cross-linked polymer with a stabilized viscosity. [Color figure can be viewed in the online issue, which is available at wileyonlinelibrary.com.]

In the viscosity versus temperature graphs of nanomodified resin and nanomodified EH (epoxy-hardener) systems represented in Figure 6, similar rheological behavior is observed. In Figure 7(a,c), the initiation of cross-linking is ~110°C for neat resin, whereas it is ~130°C for different nanorubber loadings of NBR-NP/R and CNBR-NP/R systems. Cure is delayed for about 20°C with 5 phr of nanorubber addition to the resin and the cross-linking temperature is not affected considerably with a further increase in nanorubber concentration. This delay in the exothermic curing reaction is due to the deterioration of stoichiometry within the system with nanorubber modification, which prevents further catalysis of the reaction between DICY curing agent and epoxy groups.

Table II. Cross-Linking Temperature of Nanorubber Blends

	Cross-linking temperature (°C)		
NP phr	NBR-NP/R	CNBR-NP/R	NBR-NP/EH
0	110	110	184
5	130	-	182
10	130	-	180
15	130	135	177
20	130	133	179

NP: nanoparticle, NBR-NP/R: NBR nanorubber/Resin blends, CNBR-NP/R: CNBR nanorubber/Resin blends, NBR-NP/EH: NBR nanorubber/epoxy, hardener blends without accelerator, phr: part per hundred rubber.

In Figure 7(b), in NBR-NP/EH system which does not contain accelerator, cross-linking is accelerated for about 5°C, changing from 185°C to 180°C when up to 20 phr of NBR-NP was added

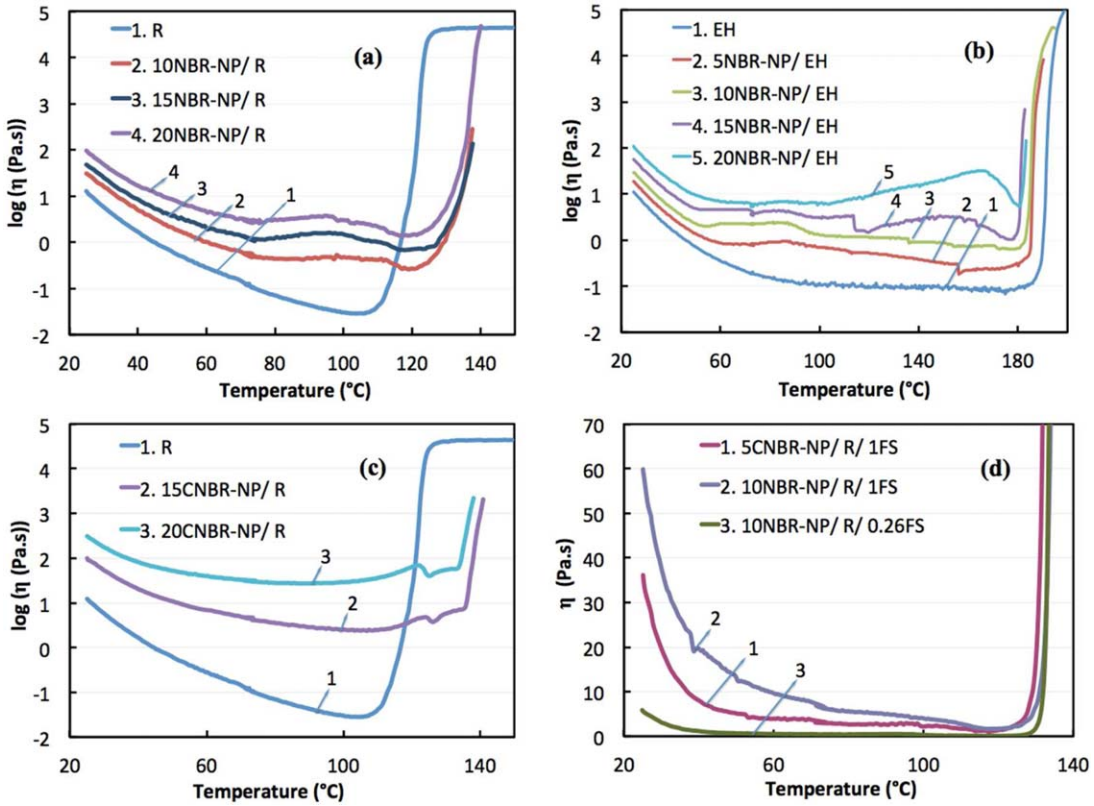

Figure 7. (a) Log(η) vs. temperature (°C) graph of NBR-NP/R blends, (b) log(η) vs. temperature (°C) graph of NBR-NP/EH blends, (c) log(η) vs. temperature (°C) graph of CNBR-NP/R blends, (d) η (Pa s) vs. temperature (°C) graph of nanorubber/R/FS systems. [Color figure can be viewed in the online issue, which is available at wileyonlinelibrary.com.]

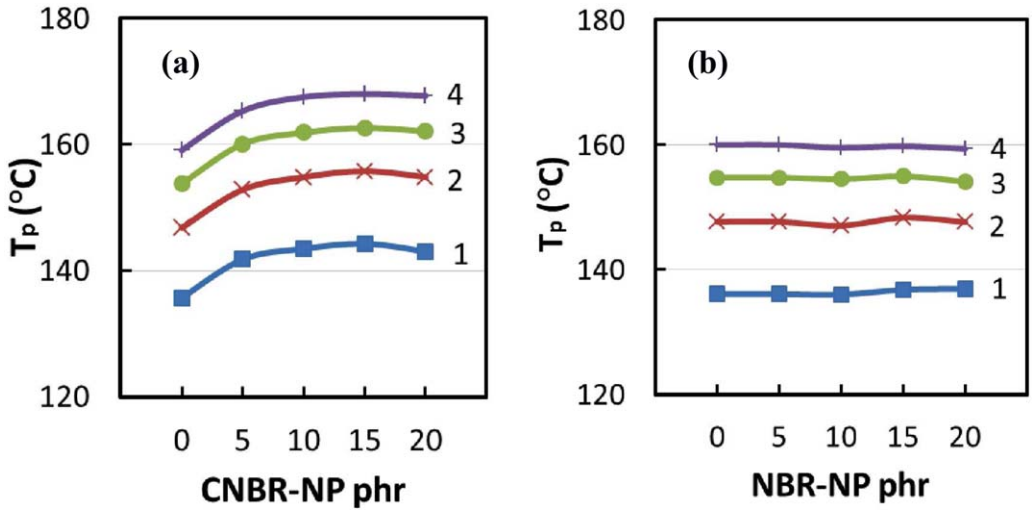

Figure 8. T_p (°C) vs. nanorubber phr for (a) CNBR-NP/R system, (b) NBR-NP/R system at different heating rates, 1: 5°C/min, 2: 10°C/min, 3: 15°C/min, 4: 20°C/min. [Color figure can be viewed in the online issue, which is available at wileyonlinelibrary.com.]

into the system. It can be clearly seen that NBR-NP catalyze the curing reaction in absence of accelerator in the system. Therefore, the function of NBR-NP in the curing reaction is similar to that of accelerators. The reason of this is attributed to two phenomena. This catalysing effect can be due to the interaction between the basic cyanide (nitrile) groups of NBR-NP and the hydroxyl groups of DGEBA resin. Fan *et al.* [3] carried out a detailed FT-IR study of a similar system and reported the same phenomenon. The second reason is a physical phenomena in which case the NBR-NP creates large amount of surface areas in the system that hold the epoxy and the curing agent together as a suspension and prevent sedimentation. Sedimentation is a main problem within DICY curing agent systems due to possible density differences because DICY is an insoluble solid paste at RT.[30,31] In a way the nanorubber can hold the system together and the huge surface area created within the matrix may act as an active surface for cross-linking. However in comparison with the accelerator, the catalytic ability of NBR-NP in the curing reaction was weaker.

In order to study the effect of fumed silica (FS) on the viscosity behavior, blends with FS loadings of 0.26 and 1 phr were studied in Figure 7(d) shows that fumed silica has no considerable effect on the cross-linking, but ~0.75 phr of fumed silica addition increased the viscosity of the 10NBR-NP/R blend by 50 Pa s at RT.

The viscosity changes reported in this section with both nanorubber and fumed silica additions are well within the processability requirements of commercial composite manufacturing techniques. This part of the study was used as a guide for an optimum cure-cycle determination and to study the processing requirements of the nanorubber modified resin systems.

Cure Analysis, Differential Scanning Calorimeter

The effect of both nanorubbers on the cure behavior of the resin is studied in this section. T_p (peak exothermic temperature) variance with nanorubber addition for both systems is given in Figure 8. In this figure, for the experiments conducted at 10°C/min, for with 5 phr of NBR-NP and CNBR-NP addition to neat resin, the T_p of the system increases by 3 and 6°C respectively.

Large specific surface area of the nanorubber particles likely induce interfacial interactions with the polymer chains and influence the thermal properties of the matrix[32] hence affect the curing reaction rate by changing the exothermic cross-linking temperature. Good dispersion of the nanorubber within the matrix leads to an interphase zone in which the mobility of the matrix polymer chains is constrained. This increase in T_p may also be attributed to the dilution phenomena within the system. As dilution within the system increases with the addition of the nanorubber, there will be a decrease in the density of the reaction groups.[33] The result is in agreement with the reported cases in literature, including that of epoxy systems modified with carboxyl-terminated butadiene acrylonitrile rubber (CTBN).[34]

The peak temperature stays stable after 5 phr of nanorubber addition for both systems, which agrees with the oscillatory shear measurements (rheological cross-linking temperatures data). This is due to creation of excess of surface area with 5 phr nanorubber addition after which the stoichiometry is not affected.

The slight difference in exothermal T_p behavior with different types of nanorubber modification is due to the difference in dispersed particle size, the distribution efficiency and the amount of surface area that nanorubbers create within the system. CNBR-NP, as it can be dispersed more evenly (observed in the SEM images), creates higher surface area, which affects the stoichiometry within the system in larger aspects. Within NBR-NP system partial agglomeration was observed due to which less active surface area was created and less deterioration in stoichiometry was observed. As a result, the delay in exothermal cross-linking was less. This phenomenon is reflected on the cross-linking activation energy (E_a) of the nanofluids as well.

In Table III, E_a values calculated using Kissinger method are slightly lower than the values calculated using Ozawa method.

Table III. Activation Energies for all Blends, Calculated with Flynn Wall Ozawa and Kissinger Technique

Activation energy, E_a (kJ/mole)		
Sample	Flynn Wall Ozawa	Kissinger
R	82	80
5NBR-NP/R	81	79
10NBR-NP/R	82	79
10NBR-NP/R/0.26 FS	82	79
15NBR-NP/R	84	82
20NBR-NP/R	87	84
5 CNBR-NP/R	85	82
10CNBR-NP/R	84	81
15CNBR-NP/R	85	83
20CNBR-NP/R	82	79

FS: Fumed silica.

There is a slight increase in E_a values with nanorubber concentration for NBR-NP blends whereas the activation energy decreases slightly with nanorubber concentration in CNBR-NP blends. Fumed silica addition within the system does not affect the activation energy.

This difference of E_a with nanorubber concentrations for these two nanorubber systems can be attributed to the single particle diameter and dispersion efficiency of the two nanorubbers within resin. Evenly dispersed CNBR-NP create larger surface area within the same amount of sample on which curing reaction takes place. With the creation of further cure initiation spots within CNBR-NP/R blends, the energy required for the reaction to start is slightly decreased. So in a way, with a decrease in the size of the particles dispersed within the matrix and higher surface energy storage, physically the cure reaction is eased.

Conversely, in NBR-NP/R blends, due to slight agglomeration and larger single particle size at high nanorubber loadings, the stoichiometry of the system is affected and the energy required to start the reaction is increased.

Dynamic Mechanical Analysis (DMA)

The fluctuation in T_g with nanorubber concentration obtained from the dynamic mechanical analysis of the laminates is shown in Figure 9(a). In this figure, it can be observed that there is a 2°C decrease in the T_g with 20 phr of NBR-NP addition to the matrix meaning a slightly less dense resin network whereas the T_g is not affected with CNBR-NP modification. T_g in CNBR-NP modified CFRP laminates increases for 2°C with 5 phr of CNBR-NP addition and decreases slightly and consistently after this loading. This initial increase in T_g is due to the strong interfacial bond between the evenly dispersed CNBR-NP and the epoxy cross-links, which modifies the polymer behavior by initializing chain entanglement. No change in T_g with CNBR-NP modification means that almost all of CNBR-NP phase is phase-separated.

For the NBR-NP modified CFRP samples, comparably larger dispersed particle diameters at high nanorubber loadings leads to rubber-rich and rubber-poor regions that help the polymer molecules move easily and thus slightly decrease the T_g.[35] As a result of the strong filler-filler interactions and weak filler-resin interactions and the lack of active polar groups at the surface, it takes efforts to blend the powdered NBR-NP with the epoxy matrix in a mechanical blender. Due to the poor compatibility of the epoxy resin with NBR-NP, there is a tendency for the nanorubber to aggregate forming a strong filler network which may do harm to the dispersion efficiency and the performance of the composites as well.[36] This decrease in T_g is also attributed to the flexibilization of the matrix. Partially dissolved NBR-NP plasticize the epoxy network. The Fox equation[37] was used to calculate the amount of NBR-NP that did not phase-separate into particles:

$$1/T_g = W_{ep}/T_{g,E} + W_{NBR\text{-}NP}/T_{g,NBR\text{-}NP} \quad (8)$$

where W is the weight fraction and the subscripts E and NBR-NP represent the epoxy and the NBR-NP, respectively. The neat epoxy polymer has a T_g of 140°C and the NBR-NP has a T_g of −17°C.[38] For the 20 phr NBR-NP toughened resin system, the Fox equation indicates that 0.8 wt % (0.95 phr) of the nanorubber does not phase-separate to give nanoparticles but remains

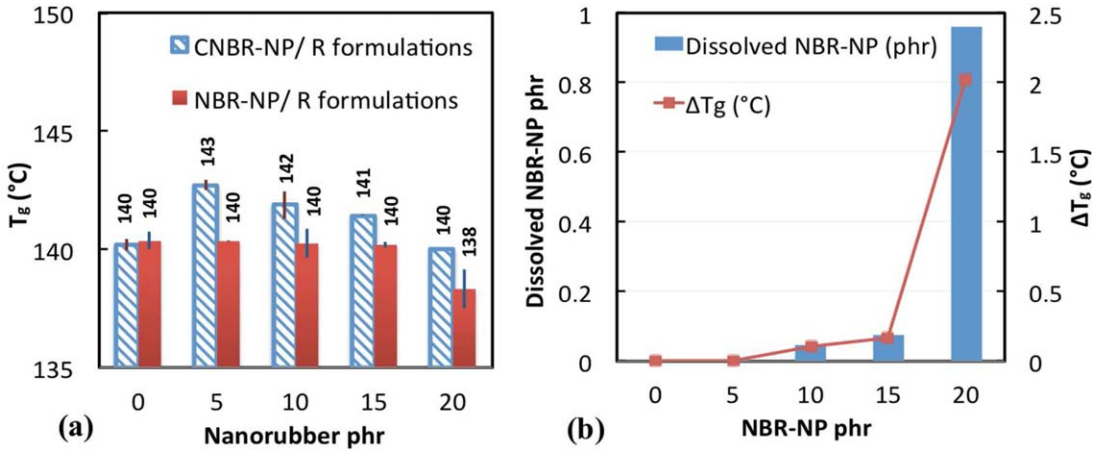

Figure 9. (a) T_g (°C) vs. Nanorubber phr for nanomodified CFRP laminates. (b) Dissolved NBR-NP phr within resin and ΔT_g (°C) vs. dispersed NBR-NP phr. [Color figure can be viewed in the online issue, which is available at wileyonlinelibrary.com.]

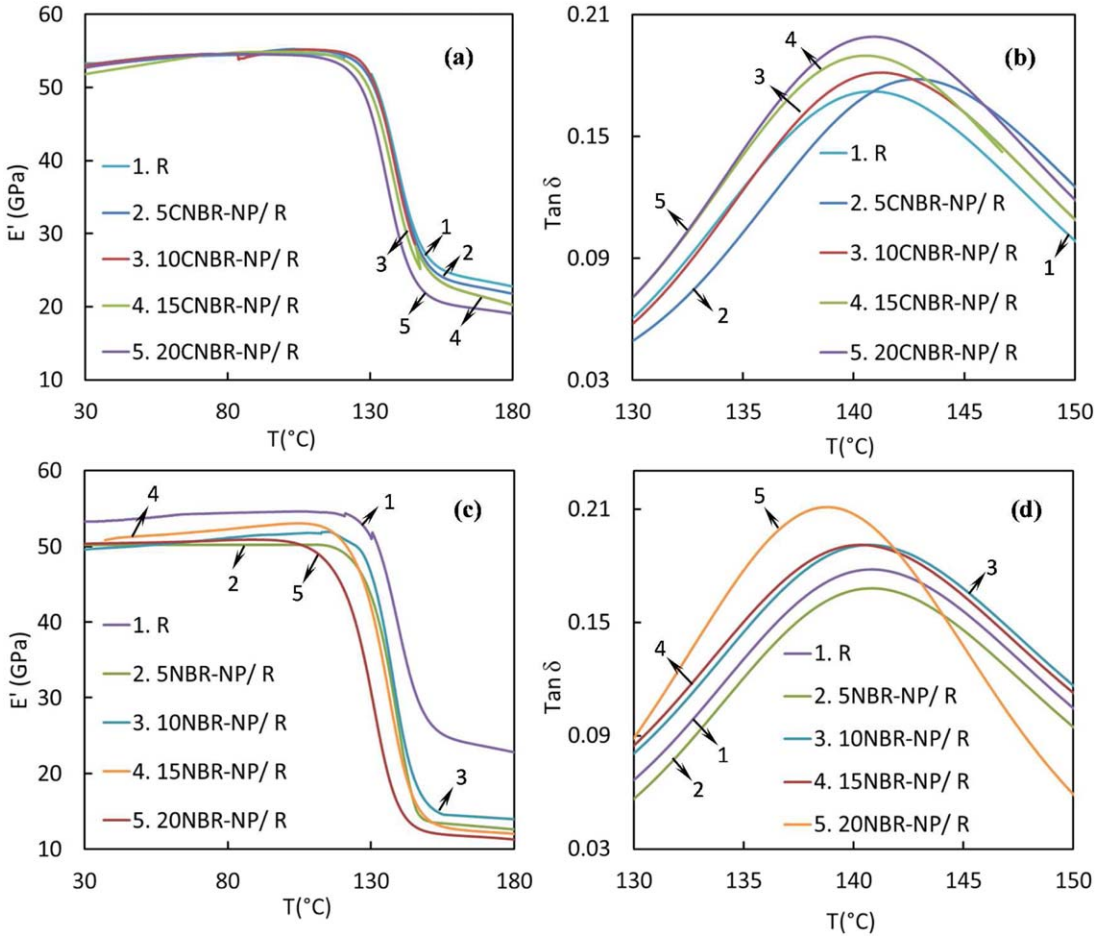

Figure 10. (a) E' (GPa) vs. T (°C) for CFRP with CNBR-NP/R matrix, (b) dynamic loss factor, tan δ vs. temperature (°C) for CFRP with CNBR-NP/R matrix, (c) E' (GPa) vs. T (°C) for CFRP with NBR-NP/R matrix, (d) dynamic loss factor, tan δ vs. temperature (°C) for CFRP with NBR-NP/R matrix. [Color figure can be viewed in the online issue, which is available at wileyonlinelibrary.com.]

in solution in the epoxy. In Figure 9(b), the dissolved NBR-NP phr and ΔT_g versus nanorubber loading is given. Until about 15 phr of NBR-NP dispersion, the amount of dissolved nanorubber phase is almost negligible however with 20 phr of nanorubber dispersion, 0.95 phr of the nanorubber does not phase separate but dissolve within the resin. This may be due to the creation of excess of surface area within the system after 15 phr of nanorubber loading which holds small amount of curing agent on the nanorubber surface and prevents further cross-linking resulting in the T_g drop.

T_g for CNBR-NP modified CFRP laminates was unchanged; since the interfacial interaction between epoxy matrix and CNBR-NP is relatively strong when compared to NBR-NP and this phenomenon can improve the mechanical properties of epoxy resin which is a continuation of this study and will be reported later. It was also observed that the T_g value was not affected by the addition of fumed silica particles.[39] Similar results, showing no change in T_g with the addition of silica particles, have been reported by other authors.[40,41]

Figure 10 shows the dynamic mechanical properties of CFRP with NBR-NP/R and CNBR-NP/R matrices. In Figure 10(a), the addition of CNBR-NP to the resin showed little influence on storage modulus over the whole temperature range. The effect of CNBR-NP on storage modulus in the glassy and the rubbery region is different. In the glassy region the storage modulus was not affected by CNBR-NP addition, which contradicts to the general expectation that the addition of a soft nanorubber should result in a decrease of the storage modulus of a stiff thermoset resin matrix. This unusual behavior can be explained in terms of the interfacial interactions due to which the local matrix mobility around the CNBR-NP is reduced. Dynamic storage modulus is also correlated with the tensile modulus of the system indicating that the CNBR-NP effectively preserves the stiffness of the polymer matrix. The slight decrease in storage modulus with an increase in nanorubber concentration in the rubbery region at elevated temperatures may be due to the dissolution of negligible amount of CNBR-NP within the matrix, resulting in slight flexibilization of the system.

In Figure 10(c) one can recognize that the incorporation of NBR-NP results in a decrease in the storage modulus over the whole temperature range compared to that of neat resin R. This issue clearly proves the plasticization effect of NBR-NP when

dispersed in the resin and a decrease in stiffness of the system respectively. Another reason to this could be the decreased degree of cross-linking induced by partial absorption of the curing agent by the nanorubber particles leading to a drop in T_g.[42,43] The storage modulus of both nanorubber formulations expresses that the nanorubber modification of the matrix decreases the temperature at which resin modulus decays.

Dynamic mechanical loss factor (tan δ) vs. temperature of neat epoxy resin and the modified networks of the two nanorubber formulations are depicted in Figure 10(b,d). The peak height of tan δ increases with increasing the nanorubber concentration for both systems. Thus, it could be concluded that the incorporation of nanorubber improves the damping behavior. Breaking intermolecular bonds with nanorubber inclusion allows greater chain mobility and results in an increase in the magnitude of tan δ peak heights.

CONCLUSIONS

In this study two novel acrylonitrile based nanorubber modified epoxy resin systems are compared to each other. The research explored a thorough story of each system starting with optimization of processing properties and requirements through rheological and curing studies. The most efficient dispersion technique was identified and the morphological properties of nanorubber modified resin matrices were studied in detail, by considering the structure/property relationships.

The SEM studies show that in higher nanorubber concentrations of NBR-NP blends, partial agglomeration occurred, and the single particle size was greater than that of CNBR-NP. Due to the plasticization effect, a 2°C decrease in T_g with 20 phr of NBR-NP addition was observed whereas CNBR-NP dispersion within the matrix did not affect the T_g. NBR-NP blends attained lower viscosity in comparison with CNBR-NP blends and both systems showed increasing shear thinning with increasing nanorubber concentration. The slight difference in activation energy (E_a) and peak temperature (T_p) in these two systems was attributed to the difference in van der Waals forces in relation to the single particle size and filler content. Inclusions of rubber caused a delay in polymerization for both systems as observed from DSC and oscillatory rheometer analysis. This is attributed to the reduction in concentration of reacting species.

Finally, it could be concluded that the two acrylonitrile based nanorubber materials do not increase the viscosity beyond processing limits 20 phr as well and do not affect the T_g of the resin substantially. Even dispersion of both nanorubbers within the resin and the good interfacial properties could improve the mechanical properties, and this will be discussed in the subsequent article.

ACKNOWLEDGMENTS

The research leading to these results has received funding from the FP7-MC-ITN under grant agreement No. 264710. The authors thank the Directorate-General for Science, Research and Development of the European Commission for financial support of the research. The authors from Kingston University, London, thank SINOPEC, Beijing Research Institute of Chemical Industry, and Cytec Industrial Materials for their kind supply of materials for the study.

REFERENCES

1. Guicun, Q.; Xiaohong, Z.; Binghai, L.; Zhihai, S.; Jinliang, Q. *Polym. Chem.* **2011**, *2*, 1271.
2. Phong, N. T.; Gabr, M. H.; Anh, L. H.; Duc, V. M.; Betti, A.; Okubo, K.; Chuong, B.; Fujii, T. *J. Mater. Sci.* **2013**, *48*, 6039.
3. Huang, F.; Liu, Y.; Zhang, X.; Gao, J.; Song, Z.; Tang, B.; Wei, G.; Qiao, J. *Sci. Chin. Ser. B Chem.* **2005**, *48*, 148.
4. Garima, T. *Mater. Sci. Eng. A* **2007**, *443*, 262.
5. Youhong, T.; Zin, Y.; Zhong, Z. *Compos. Sci. Technol.* **2013**, *86*, 26.
6. Paul, D. R.; Bucknall, C. B. Polymer Blend; Wiley: New York, **2000**; Vol.*1*, p 501.
7. Alan, G. M. U.S. Pat. 3,655,818, (**1972**).
8. Shinn-Gwo, H. *J. Polym. Res.* **2005**,*12*, 295.
9. Qian, W. *J. Appl. Polym. Sci.* **2003**, *87*, 2295.
10. Shinn-Gwo, H. *Thermochim. Acta* **2004**, *417*, 99.
11. Dalip, K. U. S. Pat. 004,863,7A1, (**2011**).
12. Widmaier, J. M. *Macromolecules* **1991**, *24*, 4209.
13. Ramanathan, T.; Abdala, A. A.; Stankovich, S.; Dikin, D. A.; Herrera Alonso, M.; Piner, R. D.; Adamson, D. H.; Schniepp, H. C.; Chen, X.; Ruoff, R. S.; Nguyen, S. T.; Aksay, I. A.; Prud'Homme, R. K.; Brinson, L. C. *Nat. Nano* **2008**, *3*, 327.
14. Anand, A.; Harshe, R.; Joshi, M. *J. Compos. Mater.* **2013**, *47*, 2937.
15. Haisheng, C.; Yulong, D.; Chunqing, T. *New J. Phys.* **2007**, *9*, 367.
16. Johannes, K. F. Reactive Polymers Fundamentals and Applications: A Concise Guide to Industrial Polymers; William Andrew: Montanuniversität Leoben, Austria **2005**.
17. Huang, F.; Liu, Y.; Zhang, X. *Sci. Chin. Ser. B. Chem.* **2005**, *48*, 148.
18. Hengyi, M.; Genshuan, W.; Yiqun, L. *Polymer* **2005**, *46*, 10568.
19. Gardner, H. C. U.S. Pat. 49,772,15A, (**1990**).
20. Jakob, A. B. *Thermochim. Acta* **1998**, *310*, 147.
21. Atarsia, A. *Polym. Eng. Sci.* **2000**, *40*, 607.
22. Ramirez, C. *J. Appl. Polym. Sci.* **2007**, *103*, 1759.
23. Nam, J.; Seferis, J. C. *J. Appl. Polym. Sci.* **1993**, *50*, 1555.
24. Ming, T.; Jibin, H.; Hanguang, W. *J. Appl. Polym. Sci.* **2011**, *124*, 1999.
25. Cox, H. L. *Br. J. Appl. Phys. 952*, 3, 72.
26. Pongdhorn, S.-Q.; Chakrit, S.; Weenusarin, I.; Puchong, T. *Adv. Polym. Technol.* **2011**, *30*, 183.
27. Hojjat, M.; Etemad, S. Gh.; Bagheri, R. *Int. Commun. Heat Mass Transfer* **2011**, *38*, 144.

28. Quemada, D. *Eur. Phys. J. Appl. Phys.* **1998**, *1*, 119.
29. Rajkumar, D. Rheology, New Concepts, Applications and Methods; **2013**, InTech: Universiti Tunku Abdul Rahman, Malaysia, Chapter 2.
30. Mark, F. F. The Effect of a Curing Agent and an Accelerator on the Glass Transition of Brominated and Unbrominated Diglycidyl Ether of Bisphenol A; Technical Report, US Army, **1998**.
31. Hagnauer, G. L.; Dunn, D. A. *J. Appl. Polym. Sci.* **1981**, *26*, 1837.
32. Fang, M.; Wang, K.; Lu, H.; Yang, Y.; Nutt, S. *J. Mater. Chem.* **2009**, *19*, 7098.
33. Jenninger, W.; Schawe, J. E. K. *Polymer* **2000**, *41*, 1577.
34. Thomas, R.; Durix, S.; Sinturel, C.; Omonov, T. *Polymer* **2007**, *48*, 1695.
35. Shen, J.; Huang, W.; Wu, L.; Hu, Y. *Compos. Sci. Technol.* **2007**, *67*, 3041.
36. Ming, Lu. *J. Nanomater.* **2010**, 2010, 352914.
37. Fox, T. G. *Bull. Am. Phys. Soc.* **1956**, *1*, 123.
38. Ming, T.; Yuan-Wang, T.; Yong, L. L.; Jinliang, Q.; Tie, L.; Li-Qun, Z. *Polym. J.* **2006**, *38*, 50.
39. Bray, D. J.; Dittanet, P.; Guild, F. J.; Kinloch, A. J. *Polymer* **2013**, *54*, 7022.
40. Baller, J.; Becker, N.; Ziehmer, M.; Thomassey, M.; Zielinski, B.; Muller, U.; Sanctuary, R. *Polymer* **2009**, *50*, 3211.
41. Liang, Y. L.; Pearson, R. A. *Polymer* **2009**, *50*, 4895.
42. Sun, L.; Warren, G.; Oreilly, J.; Everett, W.; Lee, S.; Davis, D.; Lagoudas, D. C.; Sue, H.-J. *Carbon* **2008**, *46*, 320.
43. Ma, P. C.; Kim, J.-K.; Tang, B. Z. *Compos. Sci. Technol.* **2007**, *67*, 2965.